

AI-POWERED CHEST RADIOLOGY

Medical Whitepaper

Lunit INSIGHT CXR



Perfecting Intelligence, Transforming Medicine.

About Us

Lunit, abbreviated from “learning unit,” is a medical AI software company devoted to developing advanced medical image analytics and novel imaging biomarkers via cutting-edge deep learning technology.

Founded in 2013, Lunit has been internationally acknowledged for its advanced, state-of-the-art technology and its application in medical images.

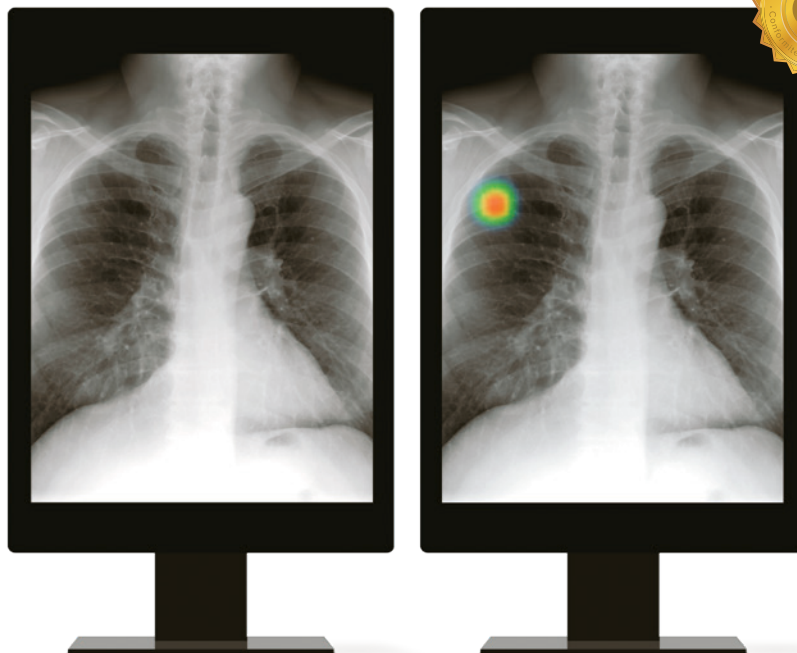
Lunit is based in Seoul, South Korea.

Our Mission

Perfecting Intelligence, Transforming Medicine.

Through our unprecedented AI technology, we seek to provide AI solutions that open a new era of diagnostics and therapeutics. We are especially focused on conquering cancer, one of the leading cause of death worldwide.

Lunit INSIGHT CXR



Lunit INSIGHT CXR

Chest radiography takes up 25% of the annual total numbers of diagnostic imaging procedures, being the most fundamental imaging test.¹ The interpretive performance, however, is suboptimal, where 20-30% are reported to be missed.²⁻³ The ever-growing burden for physicians is intensified with high volume of image to interpret.

Lunit INSIGHT CXR has been designed to solve this problem, with augmented accuracy in the detection of chest abnormalities and worklist prioritization that can enhance the workflow of a radiologist.

You can login to <https://insight.lunit.io> to freely upload images and get real-time analysis results conducted by Lunit INSIGHT in no time.

¹ Radiation UNSCotEoA. Sources and effects of ionizing radiation: sources: United Nations Publications; 2000

² Quekel LG, Kessels AG, Goei R, van Engelshoven JM. Miss rate of lung cancer on the chest radiograph in clinical practice. *Chest* 1999;115:720-4.

³ Forrest JV, Friedman PJ. Radiologic errors in patients with lung cancer. *Wes J Med* 1981;134:485.

Augmented Detection, Enhanced Workflow

With an accuracy level at 97-99%, Lunit INSIGHT CXR detects 10 radiologic findings within seconds. Moreover, to improve reading efficiency, an AI report, as pictured below, is generated upon analysis. Lunit INSIGHT CXR was trained by over 200,000 chest x-ray images.

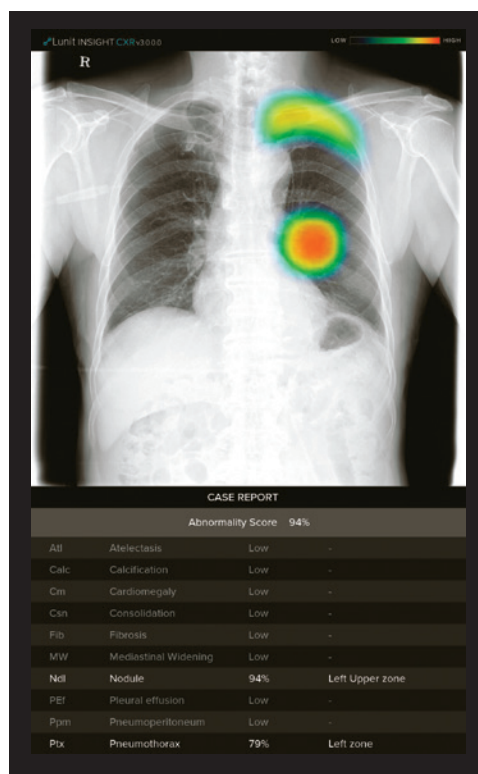
Regulatory Status (as of November 2019)

- CE: Marked
Lunit INSIGHT CXR 3 (10 Findings) - Nov. 2019
- Korea MFDS: Approved
Lunit INSIGHT CXR 1 (Nodule) - Aug. 2018
Lunit INSIGHT CXR 2 (Nodule/Mass, Consolidation, Pneumothorax) - Oct. 2019
- FDA, Japan PMDA: Expected soon.

Lunit INSIGHT CXR Analysis Report Sample

Detected Radiologic Findings:

- Atelectasis
 - Calcification
 - Cardiomegaly
 - Consolidation
 - Fibrosis
 - Mediastinal Widening
 - Nodule/Mass
 - Pleural Effusion
 - Pneumoperitoneum
 - Pneumothorax
- * TB Screening Supported



Deepen your INSIGHT with AI-Powered Chest Radiology

With the help of our AI,
you can make the best decision in less duration of time.
Together, we can save more time, save cost, and save lives.

AI Detection of Independent Chest Abnormalities on Chest Radiographs

Kim MC et al. Development of a Deep Learning-Based Algorithm for Independent Detection of Chest Abnormalities on Chest Radiographs. RSNA 2019.

Lunit INSIGHT CXR was validated internally with various dataset. Validation dataset consists of 3,671 cases from Korea and 664 cases from Europe.

Korea

Atelectasis	99.4	Mediastinal Widening	98.5
Calcification	97.7	Nodule	97.6
Cardiomegaly	98.9	Pleural Effusion	99.7
Consolidation	98.6	Pneumoperitoneum	99.9
Fibrosis	98.8	Pneumothorax	99.7
Normal vs Abnormal			97.2

Europe

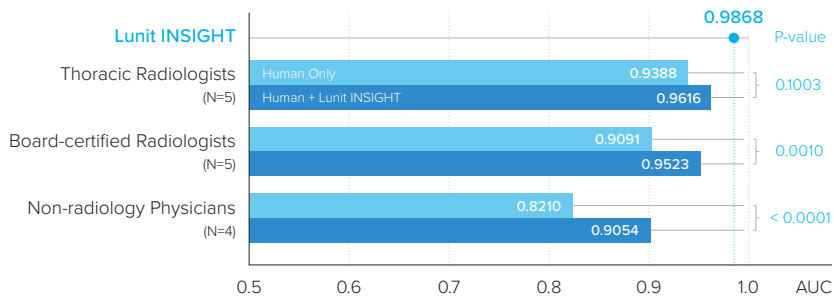
Atelectasis	96.4	Mediastinal Widening	99.6
Calcification	98.4	Nodule	96.7
Cardiomegaly	97.4	Pleural Effusion	99.6
Consolidation	99.2	Pneumoperitoneum	99.8
Fibrosis	99.4	Pneumothorax	99.9
Normal vs Abnormal			95.8

Detection of Major Chest Abnormalities with Lunit INSIGHT CXR

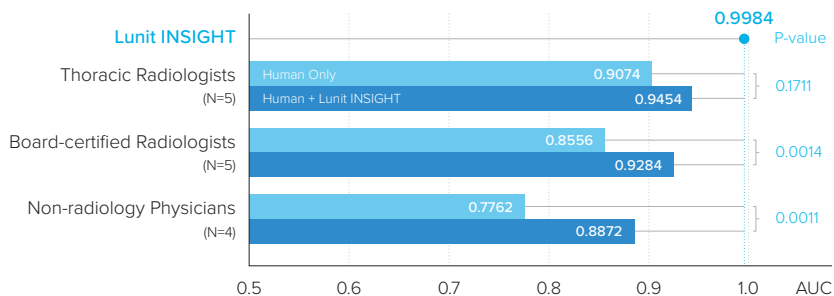
Performance Validation of a Deep Learning-Based Automatic Detection Algorithm for Major Thoracic Abnormalities on Chest Radiographs, JAMA Network Open 2019

In our efforts to clinically validate the performance level of Lunit INSIGHT CXR, we have conducted a reader study with Seoul National University Hospital. The results of this preliminary study are shown below, where the detection of major chest abnormalities (nodule/mass, consolidation, pneumothorax) has been tested in comparison to general physicians and radiologists, represented by detection of lung cancer, tuberculosis, pneumonia, and pneumothorax. The ground truth labels for the chest x-ray images used in this study were established by CT exams taken within 1 week or by consensus of an expert panel.

Detection of Major Chest Abnormalities (Image N=200)



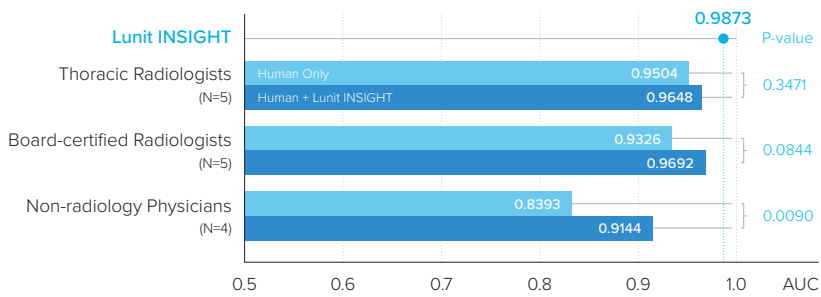
Detection of Lung Nodule (Lung Cancer) (Image N=130)



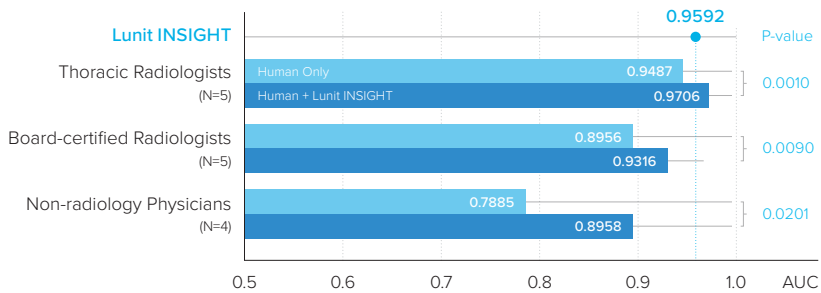
Detection of Tuberculosis (Image N=117)



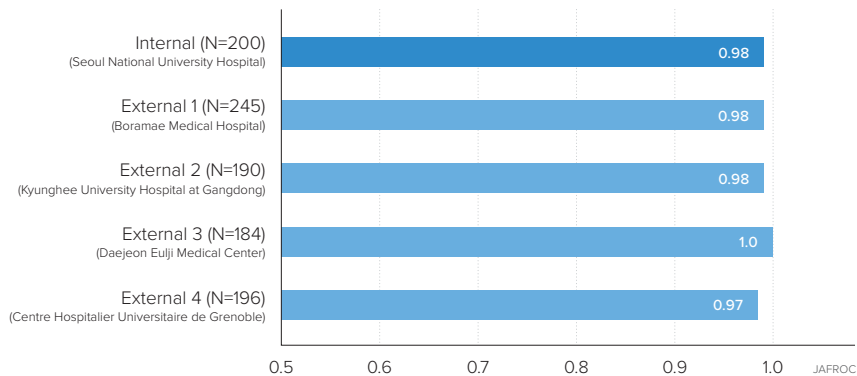
Detection of Pnuemonia (Image N=123)



Detection of Pneumothorax (Image N=121)



External Validation



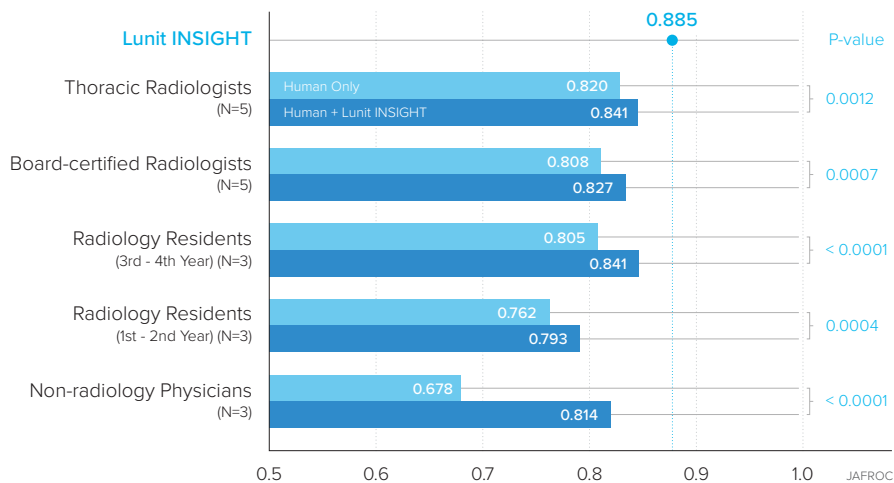
Detection of Lung Nodule with Lunit INSIGHT CXR

Nam JG*, Park SG*, et al. Development and Validation of Deep Learning-Based Automatic Detection Algorithm for Malignant Pulmonary Nodules on Chest Radiographs. *Radiology*. 2018 Sep 25:180237.

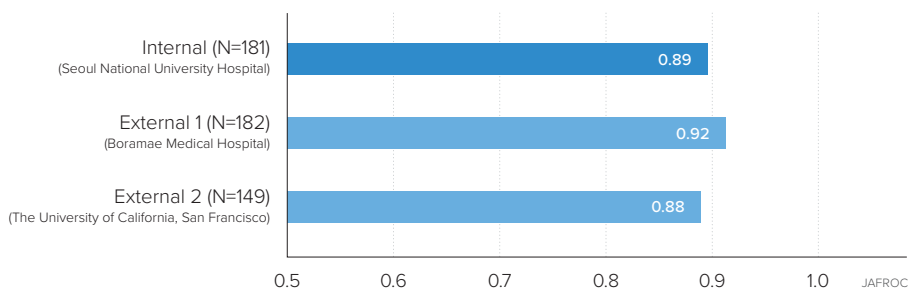
According to our reader study for detection of lung nodule in chest radiography, the accuracy of Lunit's algorithm was the highest among the entire group of readers, including thoracic radiologists and board-certified radiologists.

It has proven that with Lunit INSIGHT CXR as a second reader, physicians of different expertise level showed statistically significant increase in performance in detecting pulmonary nodules in chest x-rays. For non-radiology physicians, the performance level significantly increased up to 20%.

Accuracy in Detection of Lung Nodule



Lung Cancer External Validation



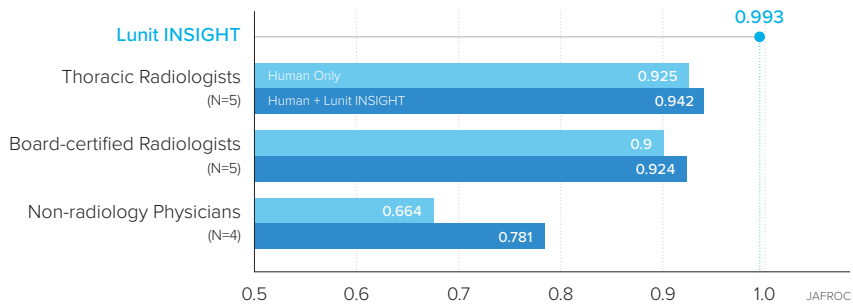
TB Screening with Lunit INSIGHT CXR

Hwang EJ*, Park SG*, et al. Development and Validation of a Deep Learning-Based Automatic Detection Algorithm for Active Pulmonary Tuberculosis on Chest Radiographs. *Clinical Infectious Diseases*. 2018 Nov 12.

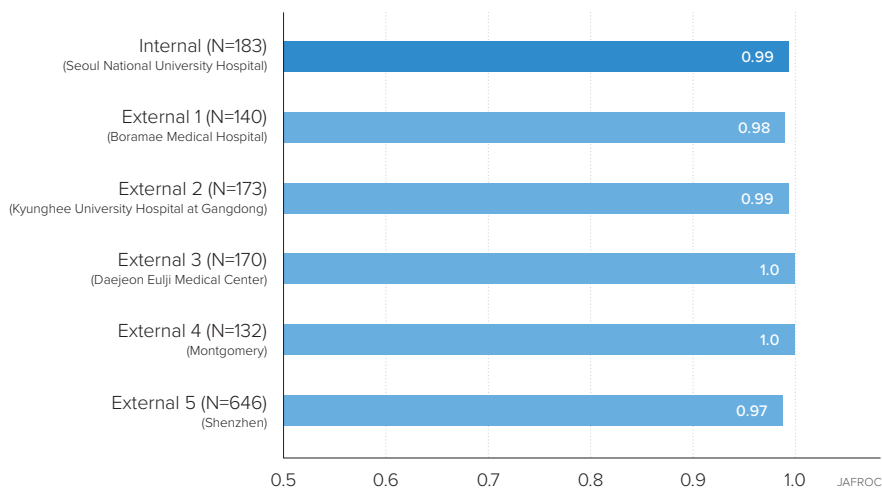
The reader study for detection of tuberculosis in chest radiography showed that Lunit INSIGHT CXR recorded the highest accuracy among 15 physicians including thoracic radiologists, non-radiology physicians, and board-certified radiologists.

It has proven that with Lunit INSIGHT CXR as a second reader, physicians showed a statistically significant increase in performance in detecting tuberculosis in chest x-rays. Moreover, Lunit INSIGHT CXR showed similar performance level with internal validation dataset when validated with external validation dataset from five different institutions, including two public dataset.

Development and Validation of Deep Learning Based Automatic Detection Algorithm for Active Pulmonary TB on Chest Radiographs



TB External Validation

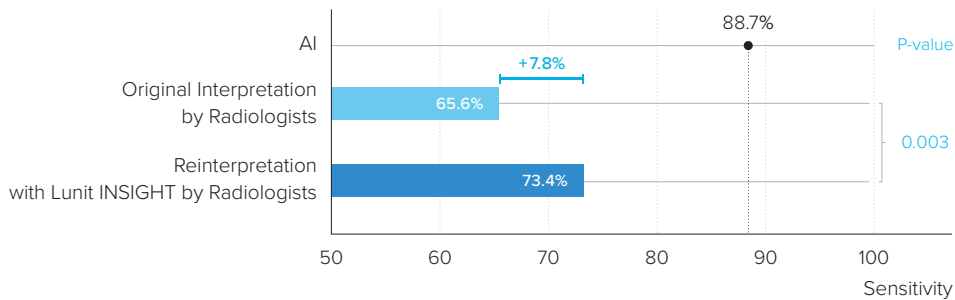


Chest X-ray Interpretation of Consecutive Patients from ER: Before and After AI Analysis

Hwang EJ et al. *Deep Learning for Chest Radiograph Diagnosis in the Emergency Department, Radiology*. 2019 Oct 22

In a chest x-ray image analysis of 1,135 consecutive patients from emergency department, Lunit INSIGHT CXR showed an AUC of 0.95 (95% CI: 0.93, 0.96) in the identification of abnormal findings.

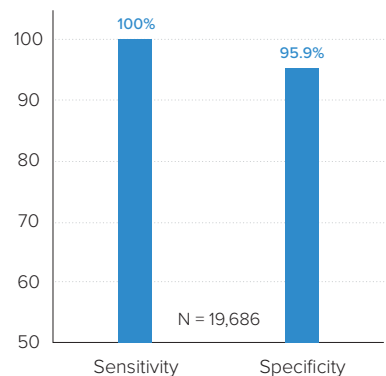
A set of chest x-ray images, with existing original interpretation conducted previously, was given to a radiology resident for a reinterpretation with Lunit INSIGHT CXR. The results showed an improvement in sensitivity (from 65.6% to 73.4%, $P = .003$) with a small reduction in specificity (from 98.1% to 94.3%, $P < .001$) upon reinterpretation with Lunit INSIGHT CXR.



Performance Validation of AI-Based Active Pulmonary TB Detection on Chest Radiographs

Lee JH et al. *Deep-Learning based Automated Detection Algorithm for Active Pulmonary Tuberculosis on Chest Radiographs: Diagnostic Performance in Systematic Screening of Asymptomatic Individuals, RSNA 2019*

To validate the TB detection performance of Lunit INSIGHT CXR, a chest x-ray image of 19,686 individuals has been gathered for analysis. All 5 active pulmonary TB cases within the individual group has been correctly detected, with 100% sensitivity and 96% specificity.

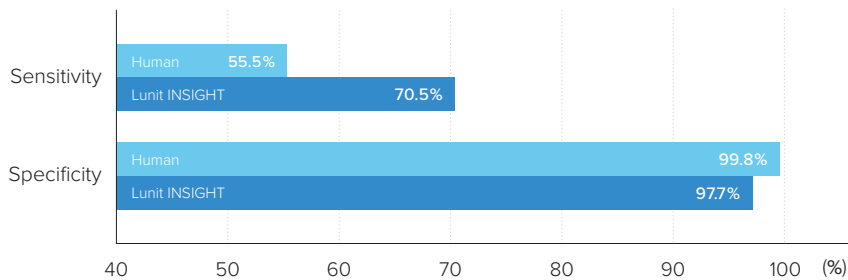


Post-Biopsy Pneumothorax Detection with AI

Hwang JH et al. Deep Learning Algorithm for Surveillance of Pneumothorax after Percutaneous Transthoracic Lung Biopsy: Validation in Multi-Center, Consecutive Cohorts, RSNA 2019

Lunit INSIGHT CXR showed outstanding performance (AUC : 0.931-0.945) for identification of pneumothorax on chest radiography, after percutaneous transthoracic needle biopsy, in consecutive cohorts from multiple institutions.

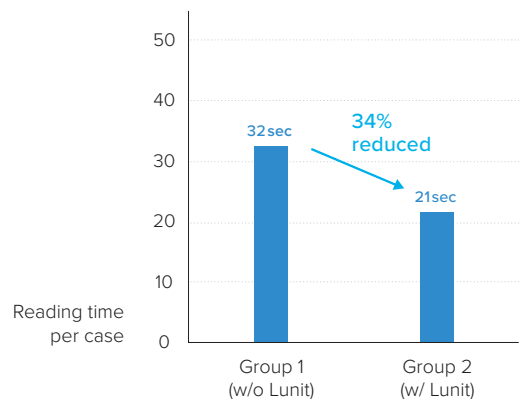
The results show that the sensitivity of Lunit INSIGHT CXR was significantly higher than that of the radiologist, at 70.5% and 55.5% respectively, while maintaining minimal difference in specificity (97.7% and 99.8%).



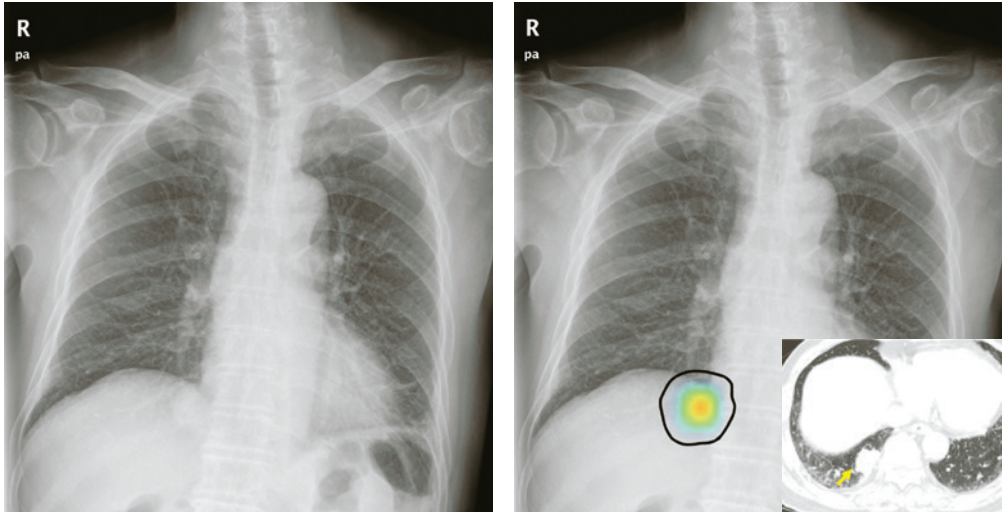
Reader Group Study Using AI-based Worklist Prioritization by Abnormality Scores

To analyze the workflow efficiency of a radiologist using Lunit INSIGHT CXR, 200 chest x-ray image data has been collected from an emergency department. Divided into 2 groups, 8 radiologists performed interpretation of chest x-ray images with and without the AI-based worklist prioritization.

Group 1 conducted normal interpretation in a randomly order, and group 2 interpreted by the order provided by AI. The results show that group 2 spent 34% less reading time than group 1.

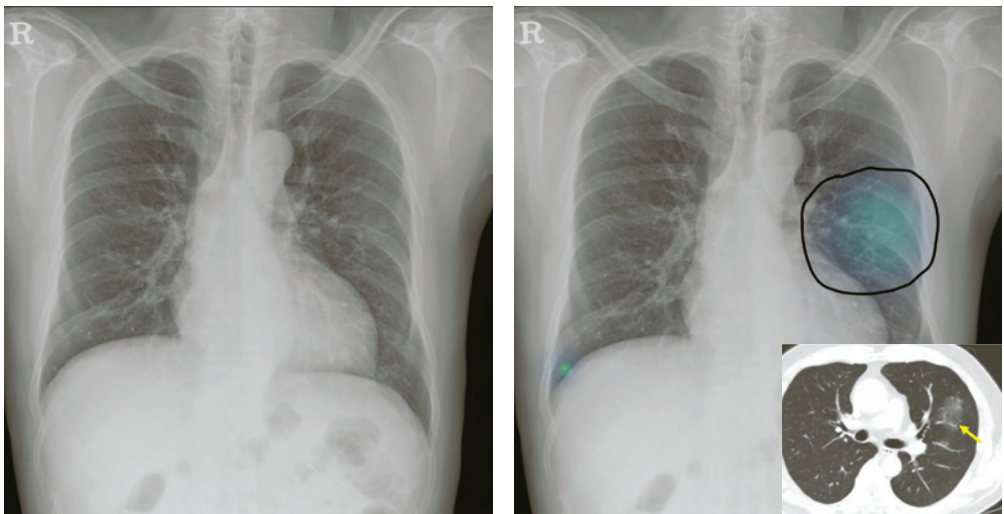


Sample Cases



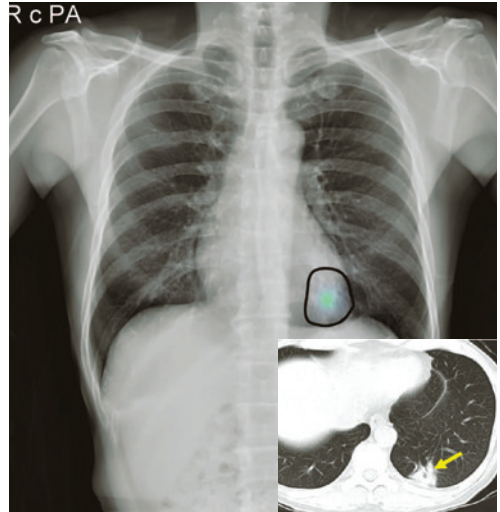
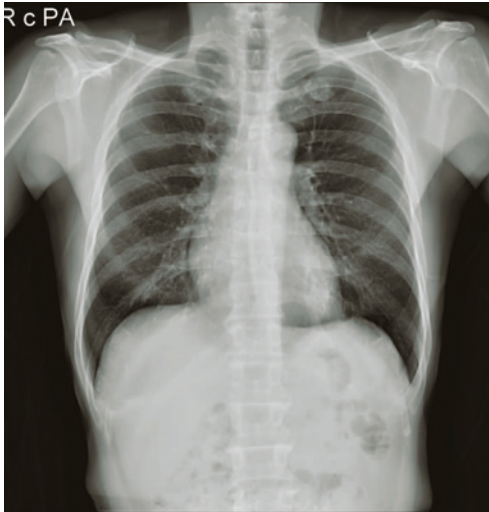
CASE 1 Lung cancer located in the right lower lobe.

Only 5 out of 10 radiologists detected this w/o Lunit. **With Lunit**, 9 were able to detect.

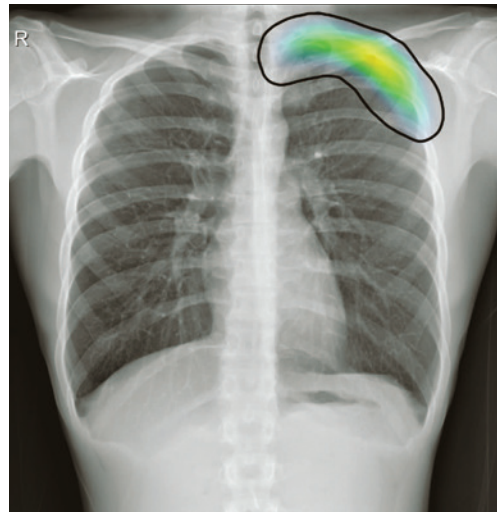
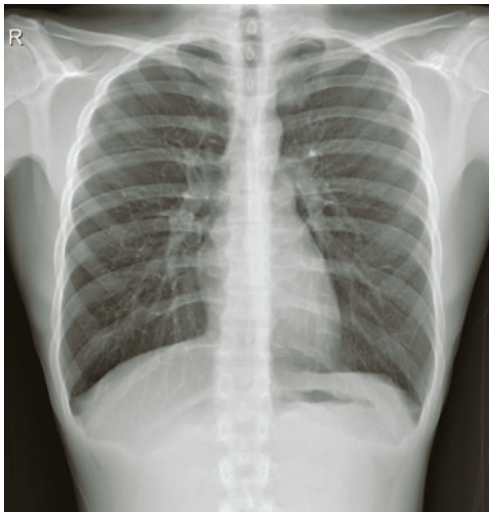


CASE 2 Pneumonia located in the left middle lung area.

None of 10 radiologists detected this w/o Lunit. **With Lunit**, 5 were able to detect.



CASE 3 Tuberculosis located in the left retrocardiac area.
7 out of 10 radiologists detected this w/o Lunit. With Lunit, all 10 were able to detect.



CASE 4 Pneumothorax at the left upper lung area.
Only 6 out of 10 radiologists detected this w/o Lunit. With Lunit, all 10 were able to detect.

Development of a Deep Learning-Based Algorithm for Independent Detection of Chest Abnormalities on Chest Radiographs

PURPOSE

To independently detect 10 abnormal radiologic findings commonly found in chest radiographs (Atelectasis, Calcification, Cardiomegaly, Consolidation, Fibrosis, Nodule, Mediastinal Widening, Pleural Effusion, Pneumoperitoneum, and Pneumothorax), we developed a deep learning based automatic detection (DLAD) algorithm and evaluated its performance with large-scale chest radiographs (CRs).

METHOD AND MATERIALS

We collected a total of 151228 CRs comprised of 79113 cases with abnormal findings (M:F=0.51:0.49; mean age=56.19±16.55). The dataset was made up of 12173 atelectasis, 1617 calcification, 4059 cardiomegaly, 7915 consolidation, 2473 fibrosis, 14422 nodule, 264 mediastinal widening, 11412 pleural effusion, 5304 pneumoperitoneum, 8286 pneumothorax, and 72115 normal cases. The dataset was randomly split into training (70353 normal, 73753 abnormal), validation (881 normal, 2680 abnormal) and test (881 normal, 2680 abnormal) sets. We developed a deep convolutional neural network with 34 layers and 16 residual connections, and it generates 10 separate 2D maps which indicate the location of each abnormality. The dataset was labeled by 18 radiologists and 16194 cases were further annotated to specify the locations of the findings. Each case in the test set has been annotated by 5 radiologists. The annotations used for the test set were taken by a majority vote. We verified the network's performance by measuring the area under the ROC curve (AUC) and jackknife alternative free-response receiver operating characteristics (JAFROC). AUC measures classification performance and JAFROC measures localization performance.

RESULTS

Our network's performance for combined abnormalities was calculated to be AUC: 0.958, JAFROC: 0.912. For the settings comparing each abnormality to the normal cases, the AUC and JAFROC were 0.983, 0.965 for atelectasis, 0.981, 0.966 for consolidation, 0.985, 0.954 for calcification, 0.984, 0.984 for cardiomegaly, 0.995, 0.988 for fibrosis, 0.971, 0.918 for nodule, 0.981, 0.978 for mediastinal widening, 0.997, 0.994 for pleural effusion, 0.999, 0.998 for pneumoperitoneum, and 0.997, 0.994 for pneumothorax.

CONCLUSION

DLAD can accurately detect and localize 10 abnormal findings in the CRs.

CLINICAL RELEVANCE STATEMENT

Since DLAD can detect abnormal findings commonly found in CRs, it can help radiologists accurately interpret various abnormalities and may also be used to distinguish between normal and abnormal CRs.

Deep-Learning based Automated Detection Algorithm for Active Pulmonary Tuberculosis on Chest Radiographs: Diagnostic Performance in Systematic Screening of Asymptomatic Individuals

PURPOSE

To validate deep-learning based automated detection (DLAD) algorithm for detection of active pulmonary tuberculosis (TB) and any radiologically-identifiable relevant abnormality on chest radiographs (CRs) in systematic screening setting.

METHOD AND MATERIALS

We performed out-of-sample testing of a trained DLAD algorithm, using CRs from 19,686 asymptomatic individuals (male: 19,475, female: 211; mean \pm standard deviation: 21.3 \pm 1.9 years) as part of systematic screening for TB between January 2013 and July 2018. Area under the receiver operating characteristic curves (AUC) of DLAD for diagnosis of TB and any relevant abnormalities were measured. Accuracy measures including sensitivities, specificities, positive predictive values (PPVs), negative predictive values (NPVs) were calculated at pre-defined operating thresholds (high sensitivity threshold, 0.16; high specificity threshold, 0.46).

RESULTS

Four individuals with five CRs were confirmed with active pulmonary TB, and 28 CRs were judged as having radiologically-identifiable relevant abnormalities in 26 individuals. All five CRs with active pulmonary TB were correctly classified as having abnormal findings by DLAD with specificities of 0.959 and 0.997, PPVs of 0.006 and 0.068, and NPVs of both 1.000 at high sensitivity and high specificity thresholds, respectively. With high specificity thresholds, DLAD showed comparable diagnostic measures for tuberculosis to the pooled radiologists (P values > 0.005). For the detection of any radiologically-identifiable relevant abnormality, DLAD showed AUC value of 0.967 (95% confidence interval, 0.938-0.996) with sensitivities of 0.821 and 0.679, specificities of 0.960 and 0.997, PPVs of 0.028 and 0.257, and NPVs of both 1.000 at high sensitivity and high specificity thresholds, respectively.

CONCLUSION

In systematic screening for TB in a low-prevalence setting, DLAD algorithm demonstrated excellent diagnostic performance, comparable to the radiologists in the detection of active pulmonary TB.

CLINICAL RELEVANCE STATEMENT

DLAD algorithm can help radiologists detect active pulmonary TB on CRs in a time-efficient manner, and identify individuals for further clinical and diagnostic evaluation for active TB. In a resource-constrained environment, it may be utilized as a standalone screening tool for individuals with active pulmonary TB.

Deep Learning Algorithm for Surveillance of Pneumothorax after Percutaneous Transthoracic Lung Biopsy: Validation in Multi-Center, Consecutive Cohorts

PURPOSE

To evaluate the performance of a deep learning algorithm (DLA) for detection of pneumothorax (PTX) after percutaneous transthoracic needle biopsy (PTNB) on chest radiograph (CR), in consecutive cohorts from multiple institutions.

METHOD AND MATERIALS

We consecutively included 1757 patients (60.0% male; median age 66 years) who underwent PTNB in 3 different institutions (Institution A:B:C=1055:388:314). We utilized a commercially-available DLA for identification of CRs with PTX. For each CR, DLA provided a probability score for the presence of PTX, along with a localization heat map. Reference standards were defined by attending thoracic radiologists of each institution. The amounts of PTX were stratified based on guidelines from the British Thoracic Society and the American College of Chest Physicians (ACCP), and percentage amount. Performance of the DLA was evaluated with area under the receiver operating characteristic curve (AUROC), sensitivities and specificities at pre-defined operating cutoff. Performance of DLA was indirectly compared with that of radiologists, by retrospective evaluation of radiology reports by radiologists in each institution.

RESULTS

PTX occurred in 17.5% (308/1757; 10.5-21.9% across institutions) of cases, among which 16.6% (51/308; 12.1-17.3% across institutions) required catheter drainage. The DLA showed AUROC of 0.937 (0.931-0.947 across institutions) for identification of PTX. Sensitivity and specificity of the DLA was 70.5% (66.8-79.1% across institutions) and 97.7% (96.3-98.5% across institutions), respectively. Radiologists showed significantly lower sensitivity (55.5%, $P < .001$) and higher specificity (99.8%, $P < .001$) than the DLA, with median turnaround time of 70.7 hours. The DLA showed 94.1% sensitivity for PTX requiring catheter drainage, and 100% sensitivities for large PTX by both guidelines and PTX with percentage amount $\geq 20\%$. Radiologists showed significantly lower sensitivities for large PTX by ACCP guideline (84.6%, $P = .046$) and PTX with percentage amount $\geq 20\%$ (87.3%, $P < .001$) than the DLA.

CONCLUSION

The DLA appropriately identified CRs with post-PTNB PTX in multi-center, consecutive cohort, with higher sensitivity than radiologists in the actual practice.

CLINICAL RELEVANCE STATEMENT

The nice performance of DLA in cohort simulating the actual clinical situation suggests potential for utilization in the practice, to help sensitive detection and timely management of post-PTNB PTX.

Partner with Us

We welcome research partnerships and other collaboration with medical institutions, healthcare providers and companies interested in implementing our software product. Currently, we have over 20 worldwide research partners throughout USA, UK, China and Korea.

We look forward to hearing from you!

Corporate Partners

The logo for FUJIFILM, featuring the word "FUJIFILM" in a bold, black, sans-serif font. A small red vertical bar is positioned above the letter "I".The Microsoft Azure logo, consisting of a square icon divided into four colored quadrants (red, green, blue, yellow) followed by the text "Microsoft Azure" in a black, sans-serif font.The Dongkook lifescience logo, featuring the text "Dongkook lifescience" in a black, sans-serif font, with "lifescience" in a green color. A small black square icon is located to the right of the text.The NVIDIA logo, featuring a green stylized eye icon above the word "NVIDIA" in a bold, black, sans-serif font.The NUANCE logo, featuring a green stylized icon above the word "NUANCE" in a bold, black, sans-serif font.The ENVOY AI logo, featuring a yellow hexagonal icon with a white geometric pattern inside, followed by the text "ENVOY AI" in a bold, black, sans-serif font.The INFINITT Healthcare logo, featuring a blue globe icon to the left of the text "INFINITT Healthcare" in a black, sans-serif font.The Hewlett Packard Enterprise logo, featuring a green horizontal bar above the text "Hewlett Packard Enterprise" in a black, sans-serif font.

Contact Us

Please feel free to email us about any inquiries or questions.

contact@lunit.io

www.lunit.io

PERFECTING INTELLIGENCE,
TRANSFORMING MEDICINE.

<https://lunit.io>